Dalton Transactions

Accepted Manuscript

This article can be cited before page numbers have been issued, to do this please use: S. Konar, U. Golla, A. Adhikary, A. K. Mondal and R. S. Tomar, *Dalton Trans.*, 2016, DOI: 10.1039/C6DT01496H.

This is an *Accepted Manuscript*, which has been through the Royal Society of Chemistry peer review process and has been accepted for publication.

Accepted Manuscripts are published online shortly after acceptance, before technical editing, formatting and proof reading. Using this free service, authors can make their results available to the community, in citable form, before we publish the edited article. We will replace this *Accepted Manuscript* with the edited and formatted *Advance Article* as soon as it is available.

You can find more information about *Accepted Manuscripts* in the Information for Authors.

Please note that technical editing may introduce minor changes to the text and/or graphics, which may alter content. The journal's standard Terms & Conditions and the Ethical guidelines still apply. In no event shall the Royal Society of Chemistry be held responsible for any errors or omissions in this *Accepted Manuscript* or any consequences arising from the use of any information it contains.

ROYAL SOCIETY OF CHEMISTRY

www.rsc.org/dalton

View Article Online
DOI: 10.1039/C6DT01496H

Journal Name

ARTICLE

Synthesis, structure, magnetic and biological activity studies of bis-hydrazone derived Cu(II) and Co(II) coordination compounds†

Received 00th January 20xx,
Accepted 00th January 20xx

DOI: 10.1039/x0xx00000x

www.rsc.org/

Upendarrao Golla,[a⊥] Amit Adhikary,[b⊥] Amit Kumar Mondal,[b] Raghuvir Singh Tomar*[a] and Sanjit Konar*[b]

Abstract: Four coordination compounds of formulae $[Cu^{II}_2(H_2L^1)(HL^1)](ClO_4)_3{\cdot}H_2O$ (**1**), $[Cu^{II}_2(H_2L^2)(CH_3OH)_2](ClO_4)_2{\cdot}2CH_3OH$ (**2**), $[Co^{II}_2(H_2L^1)_2](ClO_4)_4$ (**3**), and $[Co^{II}_2(H_2L^2)_2]{\cdot}2H_2O$ (**4**) were synthesized *via* self-assembly of succinohydrazone derived ligands (H_2L^1 = *N*′,*N*′4-bis(2-pyridyl)succinohydrazide and H_4L^2=*N*′,*N*′4-bis(2-hydroxybenzylidene)succinohydrazide) and Cu^{2+} and Co^{2+} ions respectively. Compounds were characterized by crystal structure determination, magnetic measurements and biological activities. Compounds **1**, **3** and **4** have discrete double helicate structures, whereas, compound **2** is a one-dimensional chain. Magnetic study show antiferromagnetic exchange interactions in **2** with the J value of -67.1 cm^{-1} and antiferromagnetic spin-canting in compound **3** originates through supramolecular H-bonding. For compound **3**, a nice bifurcation was observed in zero field cooled (ZFC) and field cooled (FC) measurement at the temperature of 3.5 K and the field of 0.1 T, implying long range magnetic ordering below this temperature. Interestingly, all the compounds **1**-**4** show significant changes in their absorption (hypo- and hyper chromism) in presence of SS-DNA infering interaction between compounds and DNA. In addition, compounds **1**-**4** significantly exhibited nuclease activities on both RNA and pUC19 plasmid DNA. Moreover, the nuclease activity was further enhanced in the presence of oxidant (H_2O_2) and suggests the possible role of reactive oxygen species in DNA nicking ability of compounds **1**-**4**. Furthermore, the compounds **1**, **2**, and **4** have exhibited significant cytotoxicity against mammalian cancer cell lines (HeLa, A549, and MDAMB-231). In addition, our results from Annexin/PI staining and DNA fragmentation assays revealed that these compounds are capable of inducing apoptosis and have potential to act as anticancer drugs.

Introduction

Helical structures such as deoxyribonucleic acid (DNA), α-helices in proteins exist in nature. The supramolecular helicatesare readily formed by self-assembly of ligand strands around metal ions.[1] These helicates interact with DNA, mimic artificial protein helices and can exert various biological activities. The interest on helicates significantly increased not only because of fascinating structural beauty but also promising biological activities.[2] Although a wide range of supramolecular helicates were reported with interesting magnetic and biological activities, existence of both the properties in a single system is still a challenge. Especially, metal based double-stranded or triple-stranded metallo supramolecular architectures exhibit significant cytotoxicity and have gained interest in recent years as a potential anticancer drugs.[3] Considerably, platinum and ruthenium-based binuclear double-stranded helical compounds interact with DNA, show cytotoxicity in cancer cells and emerged as possible anticancer therapeutics.[4,5] The systematic use of metal ions in assembly process facilitates to acquire specific electronic, magnetic and spectroscopic properties in the final self-assembly supramolecular helicates.[6] From magnetic point of view, both Cu (II) and Co (II) compounds are important for molecule based magnetic materials. Cu(II) has s = ½ spin and provides simplest model for magneto- structural correlation. Whereas Co^{II} ion has first order orbital contribution and strong magnetic anisotropy which helps to induce spin canting, metamagnetism, hysteresis and relaxation dynamics.[7] Origin of spontaneous magnetization may arise from the non-collinear spin arrangements on two sub-lattices of an antiferromagnet, namely spin-canting. Necessary conditions for spin-canting are (1) the presence of two non-symmetry related nearest

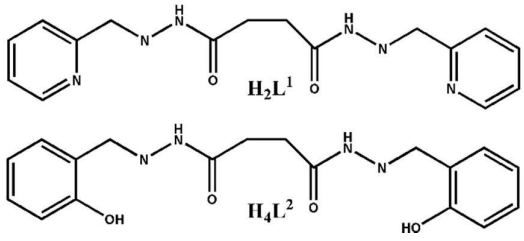

Fig. 1 Schematic drawing of the ligands H_2L^1 and H_4L^2.

[a] Department of Biological Sciences, IISER Bhopal
Fax: (+91) 755-4092392
E-mail: rst@iiserb.ac.in
[b] Department of Chemistry, IISER Bhopal
Bhopal 462066, MP (India)
Fax: (+91) 755-6692392
E-mail: skonar@iiserb.ac.in
⊥ Authors contributed equally

View Article Online
DOI: 10.1039/C6DT01496H

neighbour magnetic ions (2) antisymmetric exchange and (3) large anisotropy.[8,9] However arise of spin canting and spontaneous magnetization in a single system through weak interactions such as hydrogen bonding, π-π stacking etc. is relatively rare.[10] In addition, cytotoxicity of cobalt, copper based double-stranded helicates and their probable use for anticancer property has been reported.[11,12]

An adequate number of helicates were derived from hydrazones/hydrazides, imines, bis(bipyridine), benzimidazole and dicatechol containing ligands with different metal centres.[13] The hydrazones based ligands are highly versatile polydentate chelating agents that can form various compounds with variety of transition metals and gained the attention of many researchers. Helicate compounds of polydentate dihydrazone ligands have drawn much attention not only because of structurally importance[14], but also for their vital role in DNA binding, cytotoxic activity on human cervix carcinoma cells, tumor cell lines, etc. as well as important magnetic materials.[15] In our earlier report[16], we have explored Fe (III) metal ion containing polydentate bis-hydraozne compounds as magnetic refrigerant as well as their CT-DNA binding and dye binding abilities. In this report, a class of four metal compounds having molecular formula; $[Cu^{II}_2(H_2L^1)(HL^1)](ClO_4)_3{\cdot}H_2O$ (**1**), $[Cu^{II}_2(H_2L^2)(CH_3OH)_2](ClO_4)_2{\cdot}2CH_3OH$ (**2**), $[Co^{II}_2(H_2L^1)_2](ClO_4)_4$(**3**), and $[Co^{II}_2(H_2L^2)_2]{\cdot}2H_2O$ (**4**) has been synthesized using two flexible succinohydrazone derived ligands *N*',*N*'4-bis(2-hydroxybenzylidene)succinohydrazide (H_2L^1) and *N*',*N*'4-bis(2-pyridyl)succinohydrazide (H_4L^2) (Fig. 1) with Co^{II} and Cu^{II} ions.

Structural analysis reveals that **1** is a discrete double strand helicate and **2** is a linear chain compound where as both **3** and **4** are discrete double strand helicates. Magnetic study of **2** shows antiferromagnetic interactions between adjacent Cu^{II} centres with a J value of -67.1 cm^{-1} whereas, compound **3** is a spin-canted antiferromagnetic interaction mediated through H-bonding. Moreover, all the compounds significantly exhibited nuclease activity on both RNA and pUC19 plasmid DNA. The nuclease activity was enhanced in the presence of oxidant (H_2O_2) suggesting the possible role of reactive oxygen species in DNA nicking ability of compounds **1**-**4**. Furthermore, the compounds **1**, **2**, and **4** have exhibited significant cytotoxicity against mammalian cancer cell lines (HeLa, A549, and MDAMB-231) and are capable of inducing apoptosis. Although, all the Cu, and Co-based helicates exhibit nuclease activity on both RNA and pUC19 plasmid DNA *in vitro*, Cu-based compounds show higher cytotoxicity in human cancer cell lines. Altogether, our results show that these double-stranded supramolecular compounds of Cu have potential to act as biologically active compounds.

Experimental Section

X-ray Crystallography

Data collection of the compounds were performed at 130-140 K on a Bruker Smart Apex 2 CCD diffractometer with Mo-Kα(*λ*) 0.71073 Å) radiation using a cold nitrogen stream. Data reduction and cell refinements were performed with the SAINT program[17] and the absorption correction program SADABS[18] was employed to correct the data for absorption effects. Crystal structures were solved by direct methods and refined with full-matrix least-squares (SHELXL-2014)[19a] using WinGX[19b] and OLEX-2[19c] software with atomic coordinates and anisotropic thermal parameters for all non-hydrogen atoms.The structures of few compounds contain solvent accessible voids,hence SQUEEZE[20] module of the program suite PLATON[21] was used to generate a fresh reflection file. Although no solvent molecule has been recovered using SQUEEZE software, No. of solvent molecules in the crystal structures have been verified for compound **1** and compound **4** by TGA measurement (Fig. S1-S2). Compound **1** shows ~1.7 % wt (calculated 1.64%) in the temperature range of 23-180°C correspond to one H_2O per mole. Hence no extra solvent molecule has been added in final formulae. For compound **4**, weight loss of ~4.1 % (calculated 4.2% correspond to two H_2O per mole) was observed. Indeed two non-coordinated H_2O present in the structure. R1 and wR2 for compound **4** is slightly higher than the normal range which is due to lack of low angle reflections. Hydrogen atoms for non-coordinated water molecules could not locate which give rise B level alerts in checkcif for compound **1** and **4**. X-ray crystallographic data in CIF format is available in CCDC numbers1409570-1409573.

Materials and Methods

The reagents were used as received from Sigma Aldrich Chemicals Company. without any further purification. Magnetic susceptibility and magnetization measurements were carried out on a Quantum Design SQUID-VSM magnetometer. Direct current magnetic measurements were performed with an applied field of 0.1 T in the 1.8 K-300 K temperature range. The measured values were corrected for the experimentally measured contribution of the sample holder, while the derived susceptibilities were corrected for the diamagnetism of the samples, estimated from Pascal's tables.[9a] BVS calculations were done following the procedure given by Liu and Thorpe.[22] PXRD data were obtained with PAN analytical instrument using Cu-Kα radiation. The elemental analyses were carried out on an Elementar Micro vario Cube Elemental Analyzer. FT-IR spectra (4000–600 cm^{-1}) were recorded on KBr pellets with a Perkin Elmer Spectrum BX spectrometer.

DNA nicking assay:

For analyzing the ability of compounds to cleave pUC19 plasmid DNA, we have performed DNA nicking assay as described earlier.[23] The pUC19 plasmid was incubated at 95°C for 4 min, transferred immediately to 4°C and incubated for 20 min. The final reaction of volume of 20µL was brought up by

View Article Online
DOI: 10.1039/C6DT01496H

using 3µg of pUC19 plasmid DNA in 50mM Tris-HCl buffer (pH 7.5), and incubated along with only DMSO solvent, only 5µL of fenton's reagent (30mM H_2O_2, 50mM Ascorbic acid and 80mM $FeCl_3$) or with indicated doses of compounds, metals and ligands in presence or absence of H_2O_2 (5mM) as oxidant activator. The reaction mixtures were incubated at 37^{0}C for 2h. After the incubation, the reactions were stopped by adding DNA loading dye (0.25% bromophenol blue in 50% glycerol) and then centrifuged shortly. Finally, the reaction mixtures were loaded in 0.8% agarose gel (prepared by dissolving 0.4 g of agarose in 50 ml of 1×TAE buffer) and subjected to electrophoresis about an hour at constant voltage (90V) followed by staining with ethidium bromide. The integrity of pUC19 plasmid DNA forms was visualized by using LAS-4000 MINI gel documentation system.

Formaldehyde-Agarose (FA) Gel Electrophoresis

Total RNA was isolated from exponentially growing wild-type yeast (BY4741; *MATa his3Δ1 leu2Δ0 met15Δ0 ura3Δ0*) cells by heat/freeze phenol method as described earlier.[24] RNA was quantified by measuring A_{260} using UV-Spectrophotometer. For testing the nuclease effect of compounds on RNA, DNA-free total RNA was incubated with compounds and analyzed by denaturing FA gel electrophoresis. The final reaction volume of 20µL was brought up by using 3µg of total RNA in 50mM Tris-HCl buffer (pH 7.5), and incubated along with only DMSO solvent, only 5µL of Fenton's reagent (30mM H_2O_2, 50mM Ascorbic acid and 80mM $FeCl_3$) or with indicated doses (1, 2.5, 5, 10mM) of compounds (**1-4**), metals (M1, M2) and ligands (L1, L2). The reaction mixtures incubated at 37^{0}C for 2h were stopped by adding RNA loading dye (Saturated aqueous solution of bromophenol blue, formamide, and 20% glycerol). The samples were incubated for 10min at 65^{o}C, chilled on ice and centrifuged shortly. Finally, the reaction mixtures of RNA were resolved on 1.2% formaldehyde-agarose (FA) gel followed by staining with ethidium bromide. The integrity of RNA was visualized by using LAS-4000 MINI gel documentation system.

DNA binding experiments

In this study, Salmon Sperm Deoxyribonucleic acid (SS-DNA) was used to assess the DNA binding abilities of the compounds**1-4** by UV-Vis spectrophotometer. 5mg/ml stock solution of SS-DNA was prepared by dissolving overnight at 4^{o}C in TE buffer (10 mM Tris, pH 8.0, with 1 mM EDTA). Solutions of SS-DNA in water showed a ratio of UV absorbance at 260 and 280nm, A260/280 of 1.94 indicating that the DNA is free from proteins. Spectral titration was performed at a constant concentration of SS-DNA (50µg/mL) and by varying the concentrations (25, 50 and 75µg/mL) of compounds 1-4. The reaction volume of each 2mL was adjusted with water and the reaction mixtures were incubated at 37^{o}C for 2h with occasional mixing. Primary spectra of each was obtained by using UV-visible Spectrophotometer (Cary 100, Agilent Technologies) and imported into OriginPro 8.0 software.

Cytotoxicity Assay:

For testing the cytotoxicity potential of compounds, we have used standard MTT [3-(4,5-dimethylthiazol-2-yl)-2,5diphenyltetrazolium bromide] cell viability assay as described earlier.[11] The cell lines including human cervical cancer (HeLa), human breast adenocarcinoma (MDAMB-231), and human lung carcinoma (A549) were maintained in standard DMEM (Dulbecco's Modified Eagles' Medium) supplemented with 10% heat-inactivated fetal bovine serum at 37^{0}C in an humidified atmosphere containing 5% (v/v) CO_2. All cell lines were seeded in 96-well plate at a density of 5000 cells/well, and left undisturbed for overnight. The stock solutions of compounds including compounds (**1**-**4**), ligands (1, 2) were prepared in DMSO, whereas metals (1, 2) stock solutions were prepared by dissolving in water. The stock solutions were added in a dose range of 10-400µM in duplicate to 96-well plate and then allowed to incubate for 48h. The cytotoxicity of added compounds was evaluated by using colorimetric MTT assay. Briefly, after 48h treatment with indicated compounds, the medium was replaced with equal volume of fresh DMEM media containing a final 0.2mg/mL of MTT reagent (2mg/mL stock prepared in PBS). After 4h incubation with media containing MTT, the DMEM medium was removed and resulted formazan crystals were dissolved using DMSO solvent. Finally, the absorbance/optical density (OD) values were recorded at 570nm and 690nm.

The viability of cells was calculated as % of control as following: % of control= [(ODt-ODb)/(ODc-ODb)]*100. 'ODt' represents the mean absorbance of treated cells at 570nm, 'ODc' represents the mean absorbance of solvent treated control cells at 570nm, and 'ODb' represents the mean absorbance of respective well at 690nm. Then the dose-response curves were constructed and IC50 doses (at which the viable cells declined to 50% in treatment compared to untreated control) were calculated using GraphPad Prism (version 5) software.

Flow cytometric analysis

The perturbation in cell cycle progression of HeLa cells that were treated with IC50 dose of compounds was assessed by flow cytometric analysis as described earlier.[11] Human cervical cancer cells (HeLa) cells were seeded in 6-well plates (200,000 cells/well) in duplicate, and left undisturbed for overnight. Then the cells were left untreated or treated with IC50 doses of compounds **1**, **2**, and **4**. After 24h of incubation with compounds, the cells were trypsinized, washed once with phosphate buffered saline (PBS), and fixed with 70% ice-cold ethanol for 24h at 4^{o}C. The ethanol was removed from fixed samples by washing twice with PBS and then the samples were incubated with RNase A (1mg/mL) at 37^{o}C for 30min. Then propidium iodide (50µg/mL) was added 15min before transferring to FACS flow and analyzing DNA content by BD FACS Aria-III with BD FACS Diva software.

View Article Online
DOI: 10.1039/C6DT01496H

Apoptotic assay

The induction of apoptosis in HeLa cells treated with compound **1**, **2** and **4** was investigated by using Annexin V-FITC Apoptosis detection kit (Sigma Aldrich, India). Briefly, HeLa cells were left untreated or treated with IC50 dose of Compound **1**, **2**, and **4** for 24 or 48h and then processed according to manufacturer instructions. After 24 or 48h of treatment, cells (1×10^6 cells/mL) were washed with ice cold PBS and resuspended in 500µL binding buffer, to which 5µL of AnnexinV-FITC and 10µL of propidium iodide (PI) was added. The cells were vortexed gently and incubated in the dark for 10min at room temperature. After incubation, a minimum of 10,000 events were analyzed by using BD FACS Aria-III with BD FACS Diva software.[25]

DNA Fragmentation Assay:

DNA fragmentation assay was performed as described earlier.[26] Briefly, the HeLa cells were left untreated or treated with IC50 dose of compound **1**, **2**, and **4** for 48h in 60-mm cell culture plates. After incubation, the cells were trypsinized, harvested and washed with PBS. Then the cells were resuspended in lysis buffer (10mM Tris-HCl pH 8.0, 10mM EDTA, 0.5% TritonX-100) and centrifuged (13,000×g, 20min, 4°C) to obtain nuclei pellet, which was resuspended and incubated with DNase-free RNase A (0.1mg/mL) at 37°C for 1h. Additionally, the nuclear pellets were incubated with proteinase K (0.2mg/mL) and SDS (1%) at 50°C for 2h. The DNA from all the samples was extracted with phenol-chloroform mixture, precipitated using ethanol and ammonium acetate (pH 5.2) for 1h at -20°C. The DNA was analyzed by electrophoresis on 1.5% agarose gel and visualized by ethidium bromide staining.

Synthesis

Ligand H_2L^1 and H_4L^2 were synthesized following the previously reported procedures[27] (see supporting information).

Synthesis of $[Cu^{II}_2(H_2L^1)(HL^1)](ClO_4)_3\cdot H_2O$ **(1)**: 32.4 mg (0.1 mmol) of ligand H_2L^1 and 74.1 mg (0.2 mmol) of $Cu(ClO_4)_2\cdot6H_2O$ were taken in 10 mL of methanol in a round bottomed flask and the reaction mixture was stirred for 4 h. The solution was filtered and the filtrate was kept undisturbed for slow evaporation. After few days brown coloured single crystals suitable for X-ray diffraction were obtained from the solution. The crystals were washed with methanol and dried in air. Elemental analysis calcd.(%) for $C_{32}H_{33}Cl_3Cu_2N_{12}O_{17}$: C 35.23, N 15.40, H 3.05; found C 35.38, N 15.12, H 3.12; Selected IR data (KBr pellet; 4000 - 600 cm^{-1}): 3411(b), 2930(w), 1601(s), 1440(m), 1390(s), 1313(s), 1202(s), 1102(m), 901(m) cm^{-1}.

Synthesis of $[Cu^{II}_2(H_2L^2)(CH_3OH)_2](ClO_4)_2\cdot2CH_3OH$ **(2)**: 35.4 mg (0.1 mmol) of ligand H_4L^2 and 74.1 mg (0.2 mmol) of $Cu(ClO_4)_2\cdot6H_2O$ were taken in 10 mL of methanol in a round bottomed flask and the reaction mixture was stirred for 4 h. The solution was filtered and the filtrate was kept undisturbed for slow evaporation of the solvent. After few days blue coloured single crystals suitable for X-ray diffraction were obtained from the solution. The crystals were washed with Et_2O and dried in air. Elemental analysis calcd.(%) for $C_{22}H_{30}Cl_2Cu_2N_4O_{16}$:C 32.85, N 6.96, H 3.76; found C 32.96, N 7.01, H 3.63; Selected IR data (KBr pellet; 4000 - 600 cm^{-1}): 3425(b), 2967(w), 1601(s), 1390(s), 1301(s), 1202(s), 1085(m), 903(m), 754 (m) cm^{-1}.

Synthesis of $[Co^{II}_2(H_2L^1)_2](ClO_4)_4$ **(3):** 32.4 mg (0.1 mmol) of ligand H_2L^1 and 75 mg (0.2 mmol) of $Co(ClO_4)_2\cdot6H_2O$ were taken in 10 mL of methanol in a round bottomed flask and the reaction mixture was stirred for 4 h. The solution was filtered and the filtrate was kept undisturbed for slow evaporation of the solvent. After few days black coloured single crystals suitable for X-ray diffraction were obtained from the solution. The crystals were washed with Et_2O and dried in air. Elemental analysis calcd.(%) for $C_{32}H_{32}Cl_4Co_2N_{12}O_{21}$: C 32.56, N 14.24, H 2.73; found C 32.50, N 14.19, H 2.66; Selected IR data (KBr pellet; 4000 - 600 cm^{-1}): 3437(b), 2916(w), 1715(w), 1601(s), 1390(s), 1302(s), 1202(s), 1099(m), 903(m) cm^{-1}.

Synthesis of $[Co^{II}_2(H_2L^2)_2]\cdot2H_2O$ **(4)**: 35.4 mg (0.1 mmol) of ligand H_4L^2 and 50 mg (0.2 mmol) of $CoCl_2\cdot6H_2O$ were taken in 10 mL of methanol in a round bottomed flask and the reaction mixture was stirred for 4 h. The solution was filtered and the filtrate was kept undisturbed for slow evaporation of the solvent. After few days green coloured single crystals suitable for X-ray diffraction were obtained from the solution. The crystals were washed with Et_2O and dried in air. Elemental analysis calcd.(%) for $C_{36}H_{36}Co_2N_8O_{10}$: C 50.36, N 13.05, H 4.23; found C 48.62, N 12.71, H 3.23; Selected IR data (KBr pellet; 4000 - 600 cm^{-1}): 3437(b), 2916(w), 1601(s), 1390(s), 1302(s), 1202(s), 1099(m), 903(m) cm^{-1}.

Results and Discussion

Structural description of the compound 1

The compound **1** crystallizes in $P2_1/n$ space group in monoclinic crystal system. The asymmetric unit consists of two ligands (H_2L^1), two Cu^{2+} ions, three non-coordinated perchlorate ions and one water molecule (Fig. 2). One of the two ligand molecule is coordinated in the neutral keto form, while the other one in its mono deprotonated form.[28] BVS calculation, in the agreement with the stoichiometry of the compound give oxidation state of +2 for the copper ion (Table S1). The structural analysis reveals that ligand strands adopt C-type configuration and wraps around two Cu^{2+} by forming a double helicate cage. The dimension of the cage is approximately 4.2 x 4.6 Å^2. Flexibility of $-CH_2-CH_2-$ spacer makes the ligand bend and -C(O)-CH_2-CH_2-C(O)- moieties exhibit torsional angles of -70.3(7)° and 59.1 (7)°. Asymmetric unit of the molecule exhibits *P* helicity, however in the unit cell two independent cationic $[Cu_2L_2]^{2+}$ species of opposite chirality are present and hence results racemic solid having equal amounts of *P* and *M* helicates (Fig. S3).

View Article Online
DOI: 10.1039/C6DT01496H

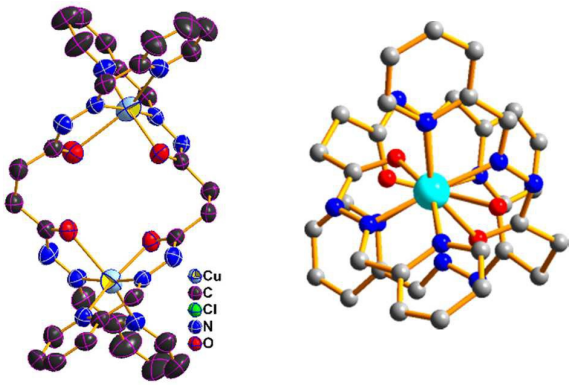

Fig. 2 Ellipsoid structure with 50% probability of compound **1** (left) and a view of compound**1** along the Cu..Cu vector emphasizing double strand helicate formation (right). Anions and solvents are omitted for clarity. Colour codes: C (grey), N (blue), O (red), Cu (cyan).

The molecule possess C2-axis passing the Cu⋯Cu centers (Fig. 2 (right)). Cu-O bond distances are in the range of 1.998(3)-2.549(3) Å. C-O distances for protonated $O_{hydrazide}$ are 1.220(7) Å, 1.238(7) Å, 1.223(8) Å and for deprotonated $O_{hydrazide}$ C-O distance is 1.278(7) Å which are in the normal range for protonated and deprotonated C-O bond distances.[29] Each of the Cu^{2+} ions are hexa-coordinated with N_4O_2 coordination environment having distorted octahedral geometry (Fig. S4). Distance between the Cu^{2+} ions is 6.273(9) Å. Cu-N bond distances are found to be in the range of 1.920-2.276 Å. The N-Cu-N, bond angles are in the range of 75.2(2)–174.0(2)° and O-Cu-O bond angles are 87.5(2)°and 88.3(2)°. The hydrazide-H (=N-NH-C(O)-) atoms involve intermolecular hydrogen bonding interactions with all the three perchlorate anions (Fig. S5). Packing diagram of compound **1** shows one dimensional arrangements of solvent water and perchlorate anions along b-axis (Fig. S6).

Structural description of compound 2

The compound **2** crystallizes in $P2_1/n$ space group in monoclinic crystal system.

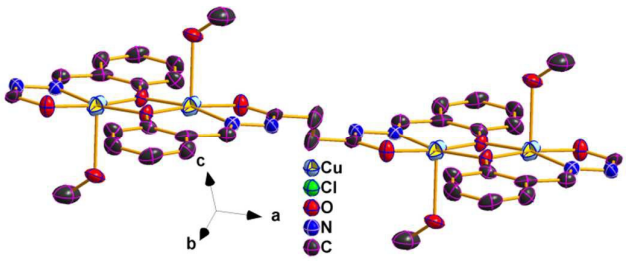

Fig. 3 Ellipsoid structure with 50% probability of compound **2**. Anions and solvents are omitted for clarity. Colour codes: C (grey), N (blue), O (red), Cu (cyan).

The asymmetric unit contains half of the ligand, one Cu^{2+} ion, one coordinated methoxy group, one non-coordinated perchlorate anion and one methanol of crystallization (Fig. 3).

The compound as a whole can be described as a one dimensional chain where -C(O)-CH_2-CH_2-C(O)- moieties of the ligand exhibits torsional angles of 180° suggesting linear configuration. Ligands exist in keto form and methoxy groups of the two adjacent metals are oriented perpendicular to each other. Molecules have an inversion center at the on -CH_2-CH_2- single bond of the ligand. Each of the Cu^{2+} ions are penta-coordinated with square pyramidal geometry having O_4N_1 coordination environment where two phenolic oxygen, one keto oxygen, one methoxy oxygen and one hydrazide nitrogen are coordinated to the metal (Fig. S8). Cu-Cu distance between two μ_2-bridged Cu^{2+} centers is 3.013(4) Å and between two dinuclear units is 8.84(1) Å. In the asymmetric unit, Cu-N bond distance is 1.95(1) Å and Cu-O bond distances are 1.97(1) Å and 1.93(7) Å. The hydrazide hydrogen (=N-NH-C(O)-) and methoxy oxygen atoms are involved in strong intermolecular hydrogen bonding interactions with perchlorate anions (Fig. S9) and solvent methanol. Packing diagram is shown in the Fig. S10. One dimensional arrangement of solvent water and perchlorate anions are illustrated in Fig. S11.

Structural description of compound 3

The compound **3** crystallizes in C2/c space group in monoclinic crystal system. The asymmetric unit contains two neutral ligands (H_2L^1), two Co^{2+} ions and four non-coordinated perchlorate ions (Fig. 4). BVS calculation suggests that the oxidation state of cobalt ion is +2 (Table S2). The structural analysis reveals that ligand strands adopt C-type configuration and wraps around two Co^{2+} ions to form a double strand helicate cage. The dimension of the cage is 4.9 x 5.1 $Å^2$. Asymmetric unit of the molecule exhibits P helicity (Fig. 4), but in its unit cell two independent cationic $[Co_2L^1{}_2]^{2+}$ species of opposite chirality are present and hence results racemic solid having equal amounts of P and M helicates (Fig. S12). C-O distances of the ligand are measured to 1.235(9) and 1.227(7) Å which are in the normal range for keto group[11] and suggests that both the ligands exist in neutral form. Each of the Co^{2+} has distorted octahedral geometry having N_2O_4 coordination environment (Fig. S13). The Co-O bond distances are found to be 2.204(4) Å and 2.170(3) Å. The Co-N bond distances are in the range of 2.04-2.13 Å. The N-Co- N, bond angles are in the range of 75.7(2)-175.0(2)° where as both the O-Co-O bond angles are 90.99 (8)°. Intramolecular Co-Co distance is found to be 6.2(9) Å. The shortest intermolecular Co⋯Co distance is measured to be 6.434 Å. The hydrazide-H atoms are involve in intermolecular hydrogen bonding interactions with the perchlorate anions and form a one dimensional chain (Fig. 5). Arrangement of solvent water and perchlorate anions in packing diagram are illustrated in Fig. S14.

View Article Online
DOI: 10.1039/C6DT01496H

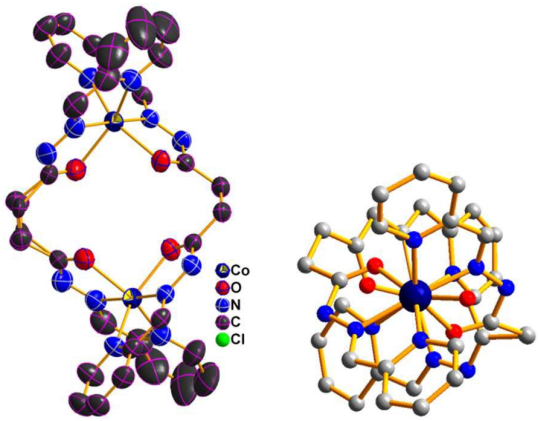

Fig. 4 Ellipsoid structure with 50% probability (left) and a view of compound **3** along the Co..Co vector emphasizing double strand helicate formation. Colour codes: C (grey), N (blue), O (red), Co (deep blue).

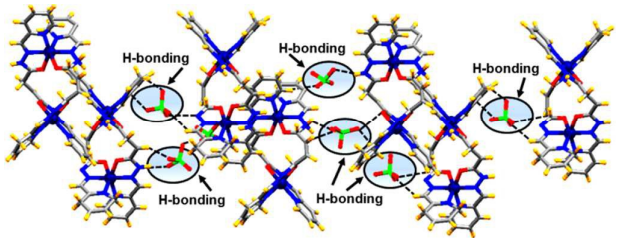

Fig. 5 Intermolecular H-bonding interactions of compound **3.**

Structural description of compound 4

The compound **4** crystallizes in $P2_1/n$ space group in monoclinic crystal system. The asymmetric unit contains two deprotonated ligands $(H_2L^2)^{2-}$, two Co^{II} ions and two non-coordinated H_2O molecules. The structural analysis reveals that ligand strands adopt C-type configuration and wraps two $Co^{2+}$by forming a double strand helicate cage. The dimension of the cage is 4.7 x 4.1 $Å^2$. Flexibility of $–CH_2$-CH_2- spacer makes the ligand bending and enables to form a double helicate. Asymmetric unit of the molecule exhibits P helicity (Fig. 6). However, in its unit cell two independent cationic $[Co_2H_2L^2{}_2]$ species of opposite chirality are present and hence results racemic solid having equal amounts of P and M helicates (Fig. S15). Each Co^{2+} ion has distorted octahedral geometry having N_2O_4 coordination environment (Fig. S16). The Co-O_{CO} bond distances are in the range of 1.92(4) - 1.93(5) Å and Co-O_{OH} bond distances lie in between 1.86(5)–1.88(5) Å. Co-N bond distances are in the range of 1.86(7)-1.88(6) Å. The intramolecular Co⋯⋯Co distance is found to be 6.04(1) Å. The hydrazide-H and phenolic oxygen atoms involve in intermolecular hydrogen bonding interaction with the chloride anions (Fig. S17).

Table 1. X-ray Crystal Data and Structure Refinement Parameters for compounds 1-4.

Compound	**1**	**2**	**3**	**4**
Formula	$C_{32}H_{33}Cl_3Cu_2N_{12}O_{17}$	$C_{11}H_{15}ClCuN_2O_8$	$C_{32}H_{32}Cl_4Co_2N_{12}O_{20}$	$C_{36}H_{36}Co_2N_8O_{10}$
Formula weight	1091.11	402.24	1164.34	858.59
T (K)	120(2)	120(2)	120(2)	120(2)
Wavelength (Å)	0.71073	0.71073	0.71073	0.71073
Space group	$P2_1/n$	$P2_1/n$	C2/c	$P2_1/n$
Crystal system	Monoclinic	Monoclinic	Monoclinic	Monoclinic
a/Å	16.9852(7)	11.627(14)	17.1541(8)	14.76(3)
b/Å	17.3596(8)	8.412(10)	17.1252(8)	15.131(3)
c/Å	17.1867(8)	16.461(18)	17.2051(9)	21.537(4)
α/deg	90	90	90	90
β/deg	107.345(3)	94.40(3)	105.721(4)	100.726(6)
γ/deg	90	90	90	90
V/Å3	4837.2(4)	1605(3)	4865.2(4)	4725.9(16)
Z	4	4	4	4
D_{calcd} (g cm-3)	1.501	1.664	1.589	1.207
μ (mm-1)	1.122	1.568	0.990	0.757
F(000)	2224	820	2400	1768
Reflection collected	5877	3547	5567	8861
Unique reflections	4535	3347	5478	6647
$^aR1, ^bwR_2$ ($I \geq 2\sigma(I)$)	0.0508, 0.1451	0.0838, 0.2629	0.0501, 0.1490	0.1026, 0.3031

$^aR_1 = \Sigma||F_o| - |F_c||/\Sigma|F_o|$; $^b wR_2 = [\Sigma w(F_o^2 - F_c^2)/\Sigma(F_o^2)^2]^{1/2}$

DOI: 10.1039/C6DT01496H

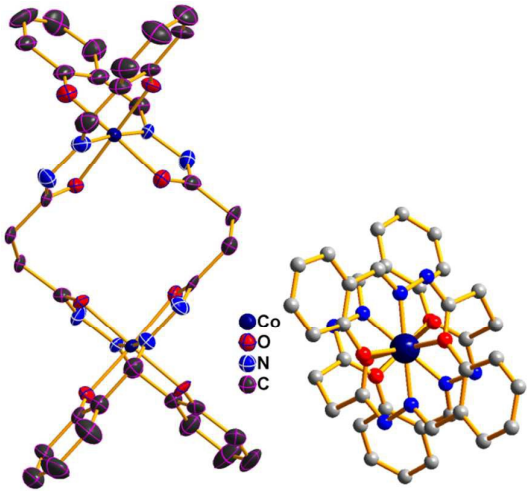

Fig. 6 Ellipsoid structure with 50% probability (left) and a view of compound **4** along the Co..Co vector emphasizing double strand helicate formation (right) of compound **4**. Colour codes: C (grey), N (blue), O (red), Co (deep blue).

Magnetic Study of compound 2

At 300 K, the observed $\chi_M T$ value is 0.73 cm^3 mol^{-1} K which is close to the spin only value of 0.75 cm^3 mol^{-1} K for two isolated Cu(II) centers (S = 1/2, g = 2.0) (Fig. 7). With decreasing temperature, $\chi_M T$ value decreases gradually and reaches to 0.005 cm^3 mol^{-1} K at 15 K and the value remains almost constant down to 2 K. The experimental $\chi_M T$ *vs*. T plot was fitted with the dinuclear model using the isotropic spin Hamiltonian (1) (inset Fig. 7). The best fit afforded g = 2.1, J = -67.1 cm^{-1} where 'J' represents interactions between the Cu(II) centers bridged through μ_2-O group and it'snegative value suggests antiferromagnetic interactions between the metal centers. Generally Cu-O-Cu bond angle for antiferromagnetic exchange should be larger than 97º.[9a] For compound **2**, Cu-O-Cu angle is 100.4(4)° which is responsible for moderate antiferromagnetic interactions.

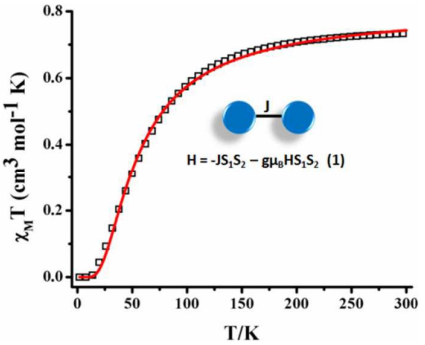

Fig. 7 Temperature dependence $\chi_M T$ plot for compound **2** measured at 0.1 T. The red solid line is best fit obtained.

Magnetic Study of compound 3

At 300 K, the observed $\chi_M T$ value is 3.42 cm^3 mol^{-1} K (Fig. 8). The value is slightly lower than the calculated spin only value of 3.75 cm^3 mol^{-1} K (g = 2) for two isolated Co (II) centers. This is mainly due to presence of inter-molecular weak antiferromagnetic interactions at 300 K.

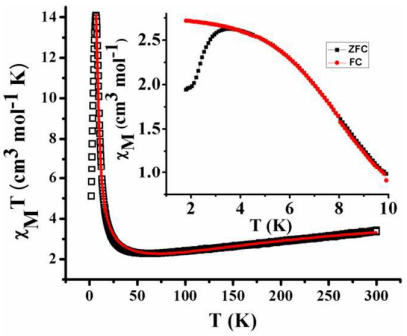

Fig. 8 Temperature dependence $\chi_M T$ plot for compound **3** measured at 0.1 T. The red solid line is best fit obtained from non-critical scaling theory.

Below 300 K, $\chi_M T$ value decreases gradually down to 2.13 cm^3 mol^{-1} K at 50 K. After that it increases sharply to attain the maximum value of 14.07 cm^3 mol^{-1} K at 6.7 K. Then $\chi_M T$ value decreases abruptly to reach to a value of 5.11 cm^3 mol^{-1} K at 1.8 K. This type of temperature dependency of $\chi_M T$ value signifies occurrence of spin-canting behavior. The sharp peak indicates existence of long range magnetic ordering. Origin of ordering is mainly due to the intermolecular hydrogen bonding (Fig. 5) along with first order orbital contribution and large anisotropy of Co^{II} ion which engenders spontaneous magnetization.[10]

Above 30K, the data was fitted from the noncritical-scaling theory with the following simple phenomenological equation (eqn (1))[30]

$\chi_M T = A \exp(-E_1/kT) + B \exp(-E_2/kT)$(1)

where, $E_1 > 0$ represents the activation energies corresponding to the spin–orbit coupling, E_2 signifies the antiferromagnetic exchange interactions, and (A + B) equals the Curie constant. The fitting gives A = 1.71 cm^3 mol^{-1} K, B = 3.16 cm^3 mol^{-1} K, E_1/k = 15.7 cm^{-1} and E_2/k = -219.03 cm^{-1}. The low E_1 value suggests little contribution of the spin–orbit coupling, and a high value of E_2 indicates significant antiferromagnetic exchange between adjacent Co^{2+} centers. To ensure spin-canting behaviour χ_M vs T were plotted from the field of 0.03 T to 0.11 T (Fig. S18). The plot shows that disappearance of the peak above 0.06 T.

These observance gives a clear indication of antiferromagnetic ordering at low temperature most likely due to field induced polarization.[31-33] Zero field cooled (ZFC) and field cooled (FC) magnetic measurements were performed at 0.1 T and a nice bifurcation was observed at the temperature of 3.5 K (inset, Fig. 8). Magnetization plot at 2 K does not show saturation even at the highest measured field of 7 T (Fig. S19). Further evidence of low temperature

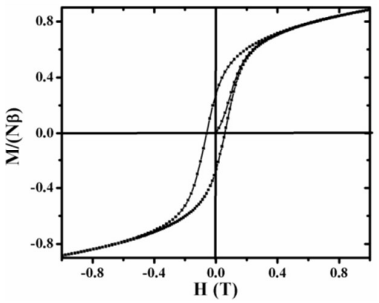

Fig. 9 Hysterisis loop for compound **3** at 2 K.

magnetic ordering was observed from field dependent isothermal magnetization measurements at 2K where a hysteresis loop was observed with a coercive field of 633 Oe and a remnant magnetization (M_R) of 0.29 Nβ (Fig. 9). The canting angle is estimated to be 2.8° using the equation $\sin(\alpha) = M_R/Ms$ (Ms = saturation magnetization).

To probe the magnetic relaxation dynamics of **3**, detailed ac magnetic susceptibility measurements were carried out in the temperature range of 1.8-10 K. In zero Oe dc field, temperature-dependent ac signals was observed (Fig. 10). However, the out-of-phase signals (χ'') do not give the peaks in the measured temperature range. Thus, to roughly estimate the energy barrier and relaxation time, another method,[34] assuming the single relaxation process of the Debye model and equation (eqn (2)), was used

$$\ln(\chi''/\chi') = \ln(\omega\tau_0) + U_{eff}/kT \qquad (2)$$

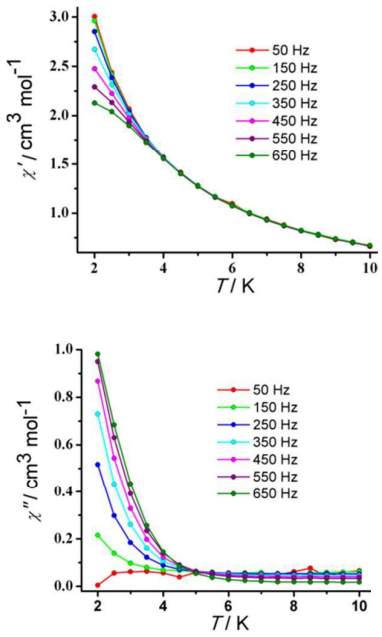

Fig. 10 Temperature dependence of the in phase (χ') (top) and out of phase (χ'') (bottom) ac susceptibility plots for compound **3** under a zero dc field.

The best fitting results give the energy barrier U_{eff} = 4.9 K and the relaxation time $\tau_0 = 7.2 \times 10^{-6}$ s (Fig. S20). Thus, the relaxation time value is consistent with the expected value of 10^{-6}-10^{-11} for a SMM.[35-37] The plot(which nature?) of χ_M'' *vs.* χ_M' known as the Cole-Cole[38] or the Argand plot (Fig. S21) is an evidence of the relaxation processes occurring in the compounds.

DNA binding study:

Usually, it is well known fact that the transition metal compounds can bind to DNA via both the covalent and/or non-covalent interactions including intercalation between the bases, groove (major/minor) binding, electrostatic and sugar-phosphate backbone binding.[39] Electronic absorption spectroscopy is a suitable method to assess the binding ability of metal compounds with DNA.[40] The DNA binding ability of Cu^{II}/Co^{II} compounds **1-4** with DNA by spectral titration of Salmon Sperm DNA (SS-DNA) with different doses of compounds. The absorption spectra of compounds **1-4** in aqueous buffer both in absence and presence of SS-DNA was shown in Fig. 11 (**2** and **4**) and Fig. S22 (**1** and **3**).

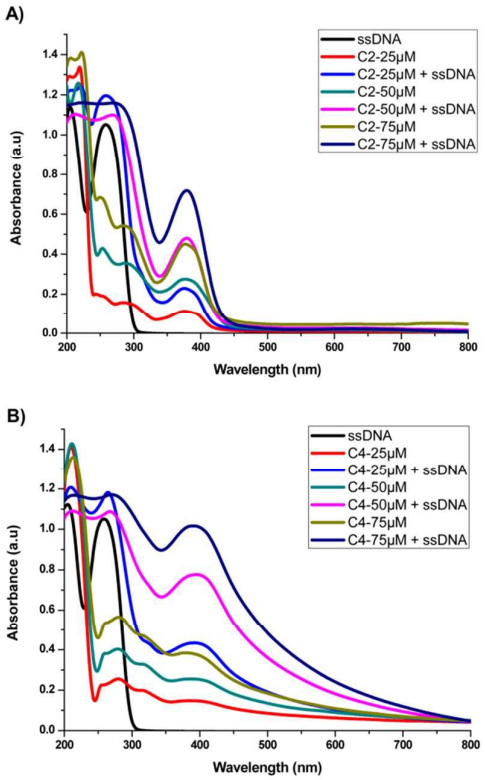

Fig. 11 UV-Visible absorption spectra of compounds **2** and **4** in the presence of SS-DNA. A & B) The compounds **2** (A) and **4** (B) of different concentrations (25, 50 and 75μM) were incubated with constant dose of SS-DNA (50μg/mL) for 2h at 37°C. The absorption spectra of SS-DNA and compounds in alone or combination were obtained by using UV-Vis spectrophotometer.

Interestingly, compound **1** exhibited hypochromic shift at 310nm whereas compounds **2**, **3**, and **4** showed hyperchromic shift in their absorption peaks at 380nm, 360nm, and 380nm respectively after addition of SS-DNA. Both the observed hypo and hyperchromic shift in absorption peak indicates the interaction of compounds with DNA.[41] Especially, the hypochromic effect indicates binding through

View Article Online
DOI: 10.1039/C6DT01496H
Journal Name ARTICLE

intercalation and staking interaction with DNA bases whereas the hyperchromic shift indicates electrostatic interaction between positively charged compound units with negatively charged phosphate backbone of DNA.[42]

In structural point of view, all the compounds **1-4** possesses a positively charged cationic unit and observed hyperchromism with compounds **2-4** in presence of SS-DNA indicates partial damage of DNA double helical structure or electrostatic interactions. To our surprise, compound **1** has showed hypochromism that might have resulted from changes in the confirmation of DNA due to intercalation. Though the complete intercalation to DNA may not be possible for dihydrazone type ligands since the ligand strands enclose metal centers, but some partial intercalation can be possible.[43] Altogether, our spectral titration results reveal the DNA binding abilities of compounds possibly through non-covalent interactions.

Nuclease activity of compounds: In recent times, the rationale for designing metal compounds that bind and cleave DNA with structural selectivity has gained interest.[44-46] The ability of compounds to cleave DNA is usually assessed by agarose gel electrophoresis of supercoiled plasmid DNA under physiological conditions. In general, circular plasmid DNA migrates faster in its supercoiled form (F1) whereas the relaxed circle forms (F3) with one strand cleaved moves very slowly. The cleavage of both the strands of plasmid DNA generates a linear form (F2), which migrates in between F1 and F3 forms. As the nuclease activity of Co (II) and Cu (II) has been well reported, the ability of our binuclear compounds to mediate DNA cleavage against pUC19 plasmid DNA was investigated under physiological conditions (pH 7.5). For testing this, one end-point nuclease activity of compounds (**1-4**), metals M1 (Cu^{2+}), M2 (Co^{2+}) and ligands L1 (H_2L^1) and L2 (H_4L^2) was performed by incubating pUC19 plasmid with 5mM of each of test compounds for 2h at 37°C. Interestingly, our agarose gel electrophoresis separation of pUC19 plasmid DNA at the end of 2h incubation with test compounds showed that all the compounds **1-4** (represented as C1-C4 in the Fig.12) exhibit nuclease activity and lost all the forms, whereas individual metals (M1, M2) and the ligands (L1, L2) retained the plasmid DNA forms at the highest concentration tested compared to untreated (C) and solvent (D) controls (Fig. 12A).

Based on our results from end-point nuclease activity, we have proceeded for further dose-dependent experimentation with only compounds. For testing dose-dependent nuclease activity of compounds, we have employed a dose range of 0.1 to 20mM. In consistent with results of end-point nuclease activity, all the compounds exhibited a maximal DNA cleavage at 2.5 to 5mM dose (lane 8, 9 respectively) and complete disappearance of supercoiled form (F1) was seen along with loss of other two forms too (Fig. 12B). Among all, compound **2** has shown significantly higher nuclease activity at 2.5mM concentration compared to other compounds tested. The loss of all forms of pUC19 plasmid DNA upon incubation with all compounds can be attributed to their higher affinity towards DNA and thus higher nuclease activity (Fig. 12B).

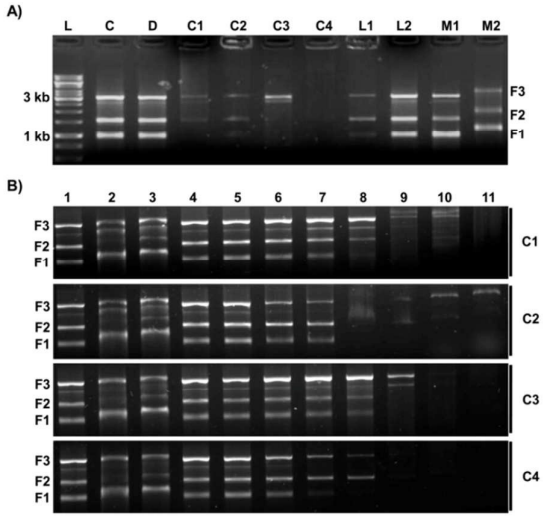

Fig. 12 Nuclease activity of compounds on pUC19 plasmid DNA. A) Agarose gel electrophoretic analysis of supercoiled (F1), linear (F2), and relaxed (F3) forms of pUC19 plasmid after incubation with 5mM of each of compounds (C**1**-C**4**), ligands (L1, L2) and metals Cu^{2+} (M1) and Co^{2+} (M2) for 2h at 37°C. Untreated (C) and DMSO solvent control (D) were served as negative controls. 'L' denotes the 1kb DNA ladder. B) Agarose gel electrophoretic analysis of supercoiled (F1), linear (F2), and relaxed (F3) forms of pUC19 plasmid after incubation with 0.1, 0.5, 1, 2.5, 5, 10, and 20mM (lanes 5, 6, 7, 8, 9, 10, and 11 respectively) of compounds (C**1**-C**4**) for 2h at 37°C. Untreated (lane 1) and DMSO solvent control (lane 4) were served as negative controls whereas fenton's reagent in alone (lane 2) or combination with DMSO solvent (lane 3) were served as positive controls.

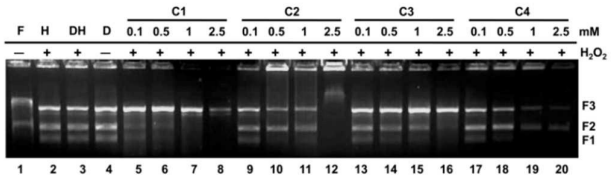

Fig. 13 Effect of oxidant (H_2O_2) on DNA nicking ability of compounds. Agarose gel electrophoretic analysis of supercoiled (F1), linear (F2), and relaxed (F3) forms of pUC19 plasmid after incubation with 0.1, 0.5, 1, and 2.5mM of compound **1** (lanes 5, 6, 7, and 8 respectively), compound **2** (lanes 9, 10, 11, and 12 respectively), compound **3** (lanes 13, 14, 15, and 16 respectively), and compound **4** (lanes 17, 18, 19, and 20 respectively) in presence of H_2O_2 (0.5mM) for 2h at 37°C. Plasmid DNA incubated with 5mM H_2O_2 (H) and DMSO solvent (D) in alone or combination (DH) (lanes 2, 4, and 3 respectively) were served as negative controls. Fenton's reagent (F) treated plasmid DNA (lane 1) was served as positive control.

The chemistry behind the DNA cleavage by metal compounds is associated with photoactivation or redox processes. In addition, the nuclease activity of metal compounds is usually influenced by the presence of activators, such as H_2O_2.[32] Further to investigate the DNA cleavage mechanism, we have incubated the pUC19 plasmid DNA with different doses of compounds in presence of H_2O_2 (5mM) as an activator. Interestingly, all the compounds exhibited pronounced nuclease activity in presence of H_2O_2 as an activator (Fig. 13).

View Article Online
DOI: 10.1039/C6DT01496H
ARTICLE
Journal Name

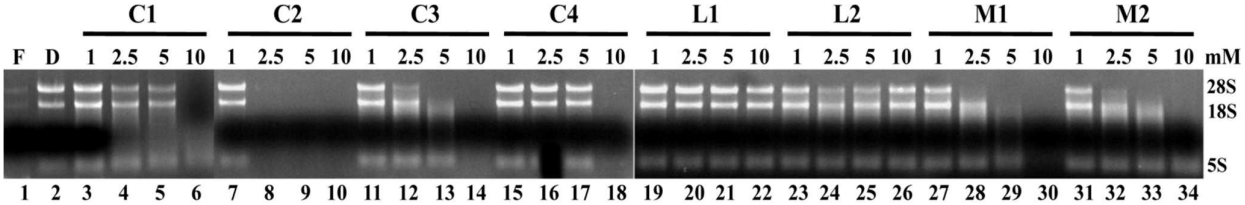

Fig. 14 Nuclease activity of compounds, ligands and metals on eukaryotic RNA. Formaldehyde Agarose gel electrophoretic analysis of total RNA (28S, 18S and 5S) from eukaryotic budding yeast after incubation with 1, 2.5, 5, 10mM of each of compounds (C**1-4**), ligands (L1, L2), metals Cu^{2+} (M1) and Co^{2+} (M2) for 2h at 37°C. DMSO solvent control (D) and Fenton's reagent (F) were served as negative and positive control respectively.

The agarose gel electrophoresis separation of pUC19 plasmid DNA forms showed clearly that the presence of oxidant (H_2O_2) have significantly increased the efficiency of compounds nuclease activity as evidenced by the disappearance of supercoiled form (F1) at very lower doses of 0.5 and 1mM (Fig. 13) compared to the results of dose-dependent activity (Fig. 12B). pUC19 plasmid incubated with known DNA cleaving Fenton's reagent (lane 1) was served as positive control, whereas plasmid incubated with DMSO solvent (D) and H_2O_2 (H) in alone or combination (DH) were served as negative controls, which eliminates the possible interference of DMSO solvent (D) with oxidant (H_2O_2). Together, our results demonstrate that all the compounds exhibit DNA cleavage activity and are redox active, which can utilize the oxidants to enhance their nuclease activity. Further studies are required to clarify the cleavage mechanisms.

As the compounds **1-4** have shown DNA nicking activity, we have asked whether these compounds can also show nuclease activity on RNA. Interestingly, all the compounds **1-4** have exhibited nuclease activity on RNA though at different doses (Fig. 14). Generally, eukaryotic RNA shows 28S, and 5S ribosomal RNA (rRNA) of 60S larger subunit whereas 18S rRNA of 40S smaller subunit on denatured FA-gel electrophoresis (lane-2, Fig. 14). Usually, the ratio of 28S/18S ribosomal RNA of >2 indicates the quality and integrity of RNA.[47] The RNA isolated from wild-type budding yeast cells showed a typical 28S/18S ribosomal RNA ratio (>2) on FA-gel electrophoresis and thus indicates that the RNA is of good quality. Further to check the nuclease effect of compounds, ligands and metals, we have incubated the total RNA with different doses at 37°C for 2h. To assess the RNA quality and integrity after 2h incubation, the reaction mixtures were checked on FA-gel electrophoresis. Interestingly, all the compounds **1-4** have showed significant nuclease activity on RNA as indicated by the loss of 28S, 18S and 5S forms of rRNA with varying affinities (lanes 3-18, Fig. 14).However, the ligands were failed to show nuclease activity (lanes 19-26, Fig. 14). Moreover, the individual metal ions also exhibited nuclease activity on major forms 28S, 18S of rRNA, not much on 5S form. Altogether, our results indicate that the compounds show significant nuclease activity on both RNA and pUC19 plasmid DNA, are redox active.

Cytotoxicity of compounds in mammalian cancer cell lines: The metal compounds exhibit significant cytotoxicity in human cancer cells and are of current interest as chemotherapeutic agents.[11,48] So, in this study we were motivated to check the cytotoxicity potential of newly synthesized Co (II) and Cu (II) based compounds against human cancer cells. To test this, we have used human cervical cancer cells (HeLa), human breast adenocarcinoma cells (MDAMB-231) and human lung carcinoma cells (A549). All the compounds (**1-4**) along with their metals (1, 2) and ligands (1, 2) were employed in a dose range of 10-400µM against all three cancer cell lines. The ability of compounds to show cytotoxicity in tested cancer cells was assessed by standard MTT [3-(4,5-dimethylthiazol-2-yl)-2,5diphenyltetrazolium bromide] cell viability assay and the results were represented in terms of IC50 values, the dose at which only 50 % of cell population is viable (Table 2). The

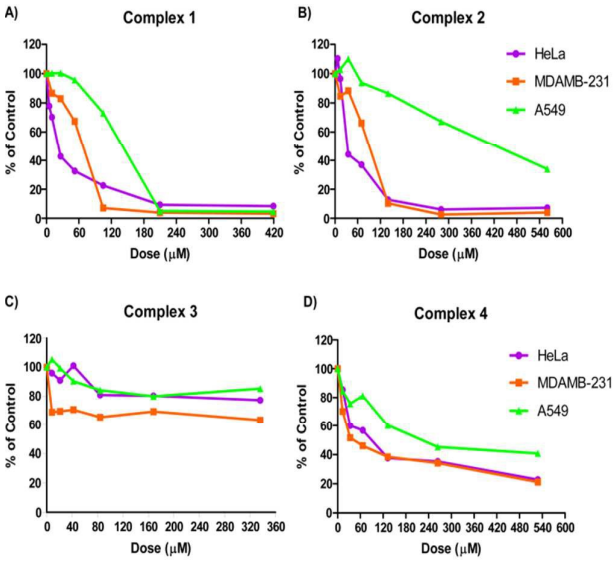

Fig. 15 The cytotoxic effect of compounds **1-4** on human tumor cell lines. A-D) The viability of human cervical cancer cells (HeLa), human breast adenocarcinoma cells (MDAMB-231), and human lung carcinoma cells (A549) treated with different doses of compounds **1** (A), **2** (B), **3** (C), and **4** (D) was measured by using typical MTT assay. The representative dose-response curves were plotted for each of cell lines and the % of viable cells was measured in comparison to untreated (DMSO) control.

View Article Online
DOI: 10.1039/C6DT01496H

Table 2. IC50 values for compounds (**1**-**4**), ligands (L1, L2) and metals (M1, M2) against mammalian cancer cell lines (HeLa, A549, MDAMB-231) after 48h of treatment.

	IC50 (μM) for Cell lines		
Compounds	**HeLa**	**MDA-MB-231**	**A549**
Compound**1**	24.42 ± 2.47	72.67 ± 8.36	133.85 ± 0.21
Compound**2**	35.73 ± 9.21	80.95 ± 1.10	388.1 ± 14.28
Compound**3**	> 360	>360	>360
Compound**4**	91.22 ± 21.04	52.85 ± 0.97	240.25 ± 37.97
Ligand 1	>400	111.72 ± 17.52	>400
Ligand 2	>400	>400	>400
Metal 1 (Cu^{2+})	143.75 ± 18.87	>400	>400
Metal 2 (Co^{2+})	>400	62.03 ± 1.51	186.55 ± 32.03

Values are represented as Mean ± SD (n=2).

representative dose-response survival curves for compounds **1-4** were shown in Fig. 15 whereas for metals and ligands were shown in Fig. S23. The compounds, metals, and ligands whose IC50 values are more than 360μM (>360) were considered as ineffective.

In all the tested compounds, only compound **1**, **2**, and **4** has shown significant cytotoxicity with little variation among the different cancer cell lines used (Table 2). The compound **3** and ligand 2 were found ineffective and didn't show any sort of cytotoxicity against any of the cancer lines tested. Metal 1 showed cytotoxicity only in HeLa cells (IC50 value is 143.75 ± 18.87), whereas metal 2 found effective against MDAMB-231 (IC50 value is 62.03 ± 1.51), A549 (IC50 value is 186.55 ± 32.03) and ligand 1 was effective only against MDAMB-231 (IC50 value is 111.72 ± 17.52). All the effective compounds **1**, **2**, and **4** show higher cytotoxicity against HeLa and MDAMB-231 compared to A549 cells (with reference to their higher IC50 values). Interestingly, the compounds **1**, **2**, and **4** conferred higher cytotoxicity against HeLa cells as evidenced by their lowest IC50 values. So, we have proceeded with HeLa cells for further experiments. Altogether, our results demonstrated that the compounds **1**, **2**, and **4** have potential to show cytotoxicity in tested cancer cells.

Effect of compounds on cell cycle: As the compounds **1**, **2** and **4** have exhibited significant cytotoxicity on human cervical cancer cells (HeLa) at lower doses compared to other cell lines tested, we have used HeLa cells for our further testing the effect of compounds on cell cycle progression. For this, HeLa cells were left untreated or treated with IC50 dose of compounds **1**, **2**, and **4** for 24h and the cell cycle progression in each condition was assessed by measuring DNA content using flow cytometry.

Interestingly, we found that the HeLa cells treated with compounds **1**, **2**, and **4** have exhibited perturbations in G1 phase of cell cycle, as seen in Fig. 16. The population of cells in G0/G1 phase of cell cycle was 49.7, 40.6, 33.3, and 42.8% of untreated, cells treated with compounds **1**, **2**, and **4** respectively. However, the perturbation of other cell cycle phases (S and G2/M) in cells treated with compounds **1**, **2**, and **4** was negligible. In addition, the cells treated with compounds **1**, **2**, and **4** have shown an increase in population of sub-G1 phase, which indicates the hypodiploid cells that have fragmented DNA (Fig. 16) and thus late apoptotic cells.[49]

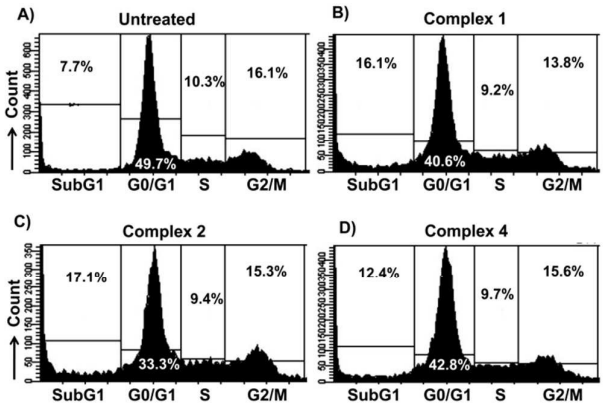

Fig. 16 Effect of compounds **1**-**4** on cell cycle progression of human cervical cancer cells (HeLa). A-D) The DNA content of HeLa cells that were left untreated (A) or treated with IC50 dose of compound **1** (B), compound **2** (C), and compound **4** (D) was analyzed by flow cytometry. The representative histograms show quantitative distribution of HeLa cells (%) in cell cycle phases.

Altogether, our results indicate that the human cervical cancer cells (HeLa) treated with compounds have perturbations in cell cycle progression and possible induction of apoptosis.

Induction of apoptosis by compounds: Cell death can be induced via necrosis and apoptosis processes. Necrosis leads to inflammation whereas apoptosis not. The induction of apoptosis in cancer cells has been used as a hallmark of assessing the ability of anticancer drugs to reduce tumor growth.[50] The significant cytotoxicity (Fig. 15) and increase in sub-G1 population (Fig. 16) of human cervical cancer cells (HeLa) motivated us to check for the induction of apoptosis upon treatment with compounds **1**, **2**, and **4**. For testing this, we have treated HeLa cells with IC50 dose of compounds and used a standard Annexin V/Propidium iodide (PI) based double dye staining method to detect cells undergoing apoptosis by flow cytometry. Basically, Annexin V is an intracellular Annexin family protein that binds specifically with phosphatidylserine (PS) in a Ca^{+2} ion dependent manner. As phosphatidylserine (PS) is externalized during early stages of apoptosis, the binding of Annexin V differentiates the apoptotic cells from normal cells.[51] In addition, the permeabilization of membrane during late stages of apoptosis and necrosis allows the entry of another dye propidium iodide (PI), which binds with nuclear DNA.[52]

View Article Online
DOI: 10.1039/C6DT01496H
ARTICLE
Journal Name

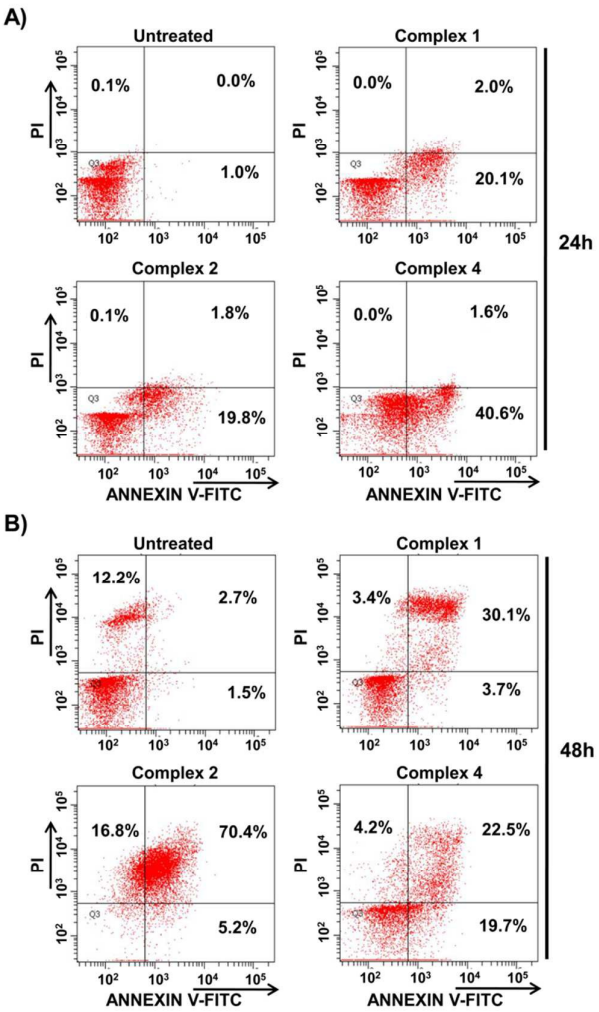

Fig. 17 Induction of apoptosis in human cervical cancer cells (HeLa) treated with compounds **1**, **2**, and **4**. A & B) Detection of apoptosis induction in HeLa cells that were left untreated or treated with IC50 dose of compounds **1**, **2** and **4** for 24h (A) and 48h (B) by flow cytometry using Annexin V/propidium iodide (PI) staining method. Viable cells (lower left quadrant) didn't bind with any dye, whereas dead cells or debris (upper left quadrant) binds only with PI. Cells in early apoptotic phase (lower right quadrant) bind only with Annexin V dye, whereas late apoptotic or necrotic cells (upper right quadrant) bind with both Annexin V and PI dyes. The value in each quadrant of dot plot shows the % of stained cells.

By this, Annexin V/PI based double dye staining method differentiates the cells in early and late stages of apoptosis. Moreover, the staining with only PI occurs in dead cells or debris and isolates from apoptotic cells. Interestingly, our flow cytometric analysis of HeLa cells that were treated with IC50 dose of compounds for 24h by Annexin V/PI staining had shown an increase in the early apoptotic cells (lower right quadrant) compared to untreated cells (Fig. 17A). In consistence, HeLa cells that were treated with IC50 dose of compounds for 48h had shown an increase in late apoptotic cells (upper right quadrant) compared to untreated cells (Fig. 17B).

The average % of cells that were stained by Annexin V and PI in alone or combination was represented in bar diagram (Fig.18A). Altogether, our results with Annexin V/PI staining had shown that the compounds (**1**, **2**, and **4**) have the potential to induce the apoptosis in human cervical cancer cells (HeLa). Apoptosis is one the fundamental cellular processes during the development and critical for assessing the cytotoxicity induced by drugs and radiation. Apoptosis in cells is characterized by fragmentation of chromosomal DNA into nucleosomal units, which results in ladder like pattern when the DNA is analyzed by agarose gel electrophoresis.[53] So, further to confirm our Annexin V/PI staining results, we have checked for DNA fragmentation in HeLa cells that were treated with IC50 dose ofcompounds (**1**, **2**, and **4**) for 48h by agarose gel electrophoresis of nuclear DNA.

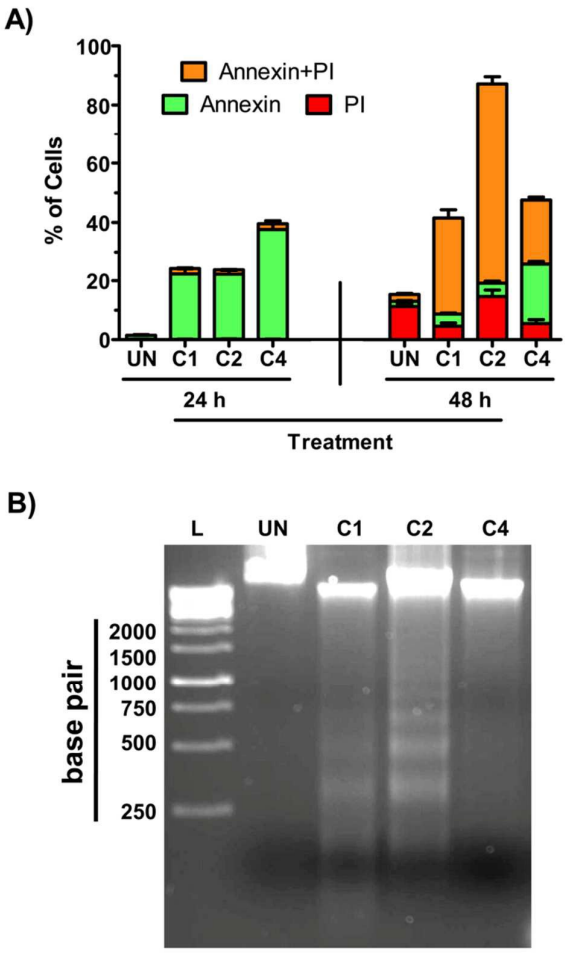

Fig. 18 Assessment of apoptosis induction in human cervical cancer cells (HeLa) treated with compounds **1**, **2**, and **4** by DNA fragmenation assay. A) Quantitave representation of human cervical cancer cells (HeLa) stained (%) in flow cytometry by only Annexin V or propidium iodide (PI) and both Annexin V/PI dyes after treatment with IC50 dose of compounds **1**, **2**, and **4** for 24h and 48h. Values are shown as Mean ± SD (n=2). B) DNA fragmentation analysis in HeLa cells treated with IC50 doses of compounds **1**, **2**, and **4** for 48h. The nuclear DNA extracted from both untreated (UN) and compounds treated HeLa cells was electrophoresed in 1.5% agarose gel and stained using ethidium bromide. 'L' denotes the 1kb DNA ladder.

Notably, HeLa cells that were treated with Compound **1** and **2** showed significant fragmentation of DNA (ladder like

pattern), whereas cells treated with compound **4** showed a minor level of nuclear DNA fragmentation compared to untreated control cells as revealed by agarose gel electrophoresis (Fig. 18B). Our DNA fragmentation results were in consistent with that of Annexin V/PI staining and suggest that the compounds **1**, **2** and **4** have the ability to induce apoptosis in human cervical cancer cells (HeLa). Altogether, our results indicate that Cu (II) based supramolecular compounds **1** and **2** have exhibited significant cytotoxicity with a low IC50 dose among the compounds tested and potential to act as antitumor agents.

Conclusions

Present study opens a new area of interplay between magnetic property as well as biological activities. Magnetic studies reveal that Compound **3** represents the first hydrazone based system and a very rare example to show H-bond mediated spin canting as well as SMM behaviour simultaneously. The biological studies unveil the cytotoxicity potential of coordination compounds as indicated by their ability to induce apoptosis in mammalian cancer cell lines. The supramolecular metal compounds also exhibited DNA binding and nuclease activities *in vitro*. The study requires further detailed investigation to understand the exact molecular mechanisms.

Acknowledgements

AA acknowledges CSIR for fellowship. AKM thanks to UGC for fellowship. UG acknowledges MHRD, India for fellowship and RST thank IISER Bhopal, CSIR and DST Government of India for financial assistance. SK thanks DAE-BRNS (project no.37(2)/14/09/2015/BRNS), Government of India for financial support. AA thanks to Srinivasulu Parshamoni for helping with the usage of latest version of SQUEEZE in crystal structure refinement. Also authors thank Dr. Himanshu Kumar, IISER Bhopal for providing mammalian cancer cell lines used in this study.

Notes and references

†Electronic Supplementary Information (ESI) available: coordination polyhedral, magnetic plots, packing arrangements, DNA binding and cytotoxicity dataare provided. See CCDC reference numbers1409570-1409573. Crystallographic data in CIF or other electronic format,DOI: 10.1039/b000000x.

1 J. M. Lehn, A. Rigault, J. Siegel, J. Harrowfield, B. Chevrier and D. Moras, *Proceedings of the National Academy of Sciences of the United States of America*, 1987, **84**, 2565.

2 (a) P. Scott and S. E. Howson, *Dalton Trans*., 2011, **40**, 10268; (b) J. Crassous, *Chem. Commun*., 2012, **48**, 9684; (c) C. Piguet, G. Bernardinelli and G. Hopfgartner, *Chem. Rev.*, 1997, **97**, 2005; (d) M. Boiocchi and L. Fabbrizi, *Chem. Soc. Rev.*, 2014, **43**, 1835; (e) M. T. Basha, J. D. Chartres, N. Pantarat, M. A. Ali, A. H. Mirza, D. S. Kalinowski, D. R. Richardson and P. V. Bernherdt, *Dalton Trans.*, 2012, **41**, 6536; (f) C. He, Y. Zhao, D. Guo, Z. Lin and C. Duan, *Eur. J. Inorg. Chem.*, 2007, 3451; (g) C. Piguet, M. Borkovec, J. Hamacek and K. Zeckert, *Coord. Chem. Rev.*, 2005, **249**, 705; (h) C. A. Schalley, A. Lutzen and M. Albrecht, *Chem. – Eur. J.*, 2004, **10**, 1072.

3 M. Albrecht, *Nature Chem*.,2014, **6**, 761.

4 A. C. Hotze, B. M. Kariuki and M. J. Hannon, *Angew. Chem. Int. Ed*.,2006, **45**, 4839.

5 T. C. Johnstone, G. Y. Park and S. J. Lippard, *Anticancer research*,2014, **34**, 471.

6 Lehn, J.-M. *Supramolecular Chemistry*; VCH: Weinheim, 1995.

7 (*a*) M. Idešicová, J. Titiš, J. Krzystek and R. Boča, *Inorg. Chem*.,2014, **53**, 2367; (*b*) F. Habib, O. R. Luca, V. Vieru, M. Shiddiq, I. Korobkov, S. I. Gorelsky, M. K. Takase, L. F. Chibotaru, S. Hill, R. H. Crabtree and M. Murugesu, *Angew. Chem. Int. Ed.,*2013, **52**, 11290; (*c*) M. G. F. Vaz, R. A. A. Cassaro, H. Akpinar, J. A. Schlueter, P. M. Lahti and M. A. Novak, *Chem. Eur. J.,*2014, **20**, 5460; (*d*) Z.-S. Cai, M. Ren, S.-S. Bao, N. Hoshino, T. Akutagawa and L.-M. Zheng, *Inorg. Chem*.,2014, **53**, 12546; (*e*) J. Boonmak, M. Nakano, N. Chaichit, C. Pakawatchai and S. Youngme, *Inorg. Chem*.,2011, **50**, 7324; (*f*) X.-H. Zhang, Z.-M.Hao and X.-M. Zhang, *Chem. Eur. J*.,2011**, 17**, 5588; (*g*) K. Mitsumoto, T. Shiga, M. Nakano, M. Nihei, H. Nishikawa and H. Oshio, *Eur. J. Inorg. Chem.*,2008, 4851; (*h*) A. K.Mondal, V. S.Parmar, S. Biswas and S.Konar, *Dalton Trans*., 2016, **45**, 4548;(*i*) L.-H. Jia, Y.-J. Wang, C. Gao, M. Ding, J.-H. Jia, B.-W. Wang and S. Gao, *Chem. Asian J.*,2014, *9*, 2463.

8 (*a*) S. Goswami, A. Adhikary, H. S. Jena, S. Biswas and S. Konar, *Inorg. Chem*.,2013**, 52**, 12064;**(***b*) X. Yang, S. Bao, M. Ren, N. Hoshino, T. Akutagawa and L. Zheng, *Chem. Commun.*,2014, **50**, 3979; (*c*) M. B. Salah, S. Vilminot, G. Andre, F. Bouree-Vigneron, M. Richard-Plouet, T. Mhiri and M. Kurmoo, *Chem. Mater*.,2005, **17,** 2612; (*d*) M. H. Zeng, W. X. Zhang, X. Z. Sun and X. M. Chen, *Angew. Chem., Int. Ed.*,2005, **44**, 3079; (*e*) Y. Z. Zhang, S. Gao, H. L.Sun, G. Su, Z. M. Wang and S. W. Zhang, *Chem. Commun*.,2004, 1906; (*f*) H-P. Jia, W. Li, Z-F. Ju and J. Zhang,*Chem. Commun*.,2008, 371; (*g*) E.-Q. Gao, P.-P. Liu, Y.-Q. Wang, Q. Yue and Q.-L. Wang,*Chem. Eur. J.***,**2009, **15**, 1217; (*h*) S. M. Humphrey, A. Alberola, C. J. Go´mezGarcı´ and P. T. Wood,*Chem. Commun*.,2006, 1607.

9 (*a*) O. Kahn, *Molecular Magnetism*; Wiley-VCH: New York, 1993; (*b*)X.-Y. Wang, Z.-M. Wang and S. Gao, *Inorg. Chem*.,2008, **47**, 5720; (*c*) A. V. Palii, O. S. Reu, S. M. Ostrovsky, S. I. Klokishner, B. S. Tsukerblat, Z-M Sun, J-G. Mao, A. V. Prosvirin, H-H. Zhao and K. R. Dunbar,*J. Am. Chem. Soc*.,2008, **130**, 14729; (*d*) Q. Zhang, H. Zhang, S. Zeng, D. Sun and C. Zhang, *Chem. Asian J.***,**2013, **8**, 1985; (*e*) T. Shiga, T. Matsumoto, M. Noguchi, T. Onuki, N. Hoshino, G. N. Newton, M. Nakano and H. Oshio, *Chem. Asian J.*,2009, **4**, 1660; (*f*) T. J. Woods, M. F. B.-Rivas, S. M. Ostrovsky, A. V. Palii, O. S. Reu, S. I. Klokishner and K. R. Dunbar, *Chem. Eur. J.*,2015, **21**, 10302.

10 (*a*) M. Ding, B. Wang, Z. Wang, J. Zhang, O. Fuhr, D. Fenske and S. Gao, *Chem. Eur. J.*,2012, **18**, 915; (*b*) D. J. Price, S.t R. Batten, B. Moubaraki and K. S. Murray, *Polyhedron,*2003, **22**, 2161; (*c*) W. X. Zhang, T. Shiga, H. Miyasaka and M. Yamashita, *J. Am. Chem. Soc*.,2012, **134**, 6908; (*d*) J. H. Yoon, D. W. Ryu, H. C. Kim, S. W. Yoon, B. J. Suh and C. S. Hong, *Chem. Eur. J.*,2009, **15**, 3661; (*e*) Q. Chen, M.-H. Zeng, Y.-L. Zhou, H.-H. Zou andM. Kurmoo, *Chem. Mater*.,2010, **22**, 2114; (*f*) K. Bernot, J. Luzon, R. Sessoli, A. Vindigni, J. Thion, S. Richeter, D.Leclercq, J. Larionovaand A. van der Lee, *J. Am. Chem. Soc*.,2008, **130**, 1619.

View Article Online
DOI: 10.1039/C6DT01496H
ARTICLE
Journal Name

11 R. Eshkourfu, B. Cobeljic, M. Vujcic, I. Turel, A. Pevec, K. Sepcic, M. Zec, S. Radulovic, T. Srdic-Radic, D. Mitic, K. Andjelkovic and D. Sladic, *J. Inorg. Biochem*.,2011, **105**, 1196.
12 D. D. Li, J. L. Tian, W. Gu, X. Liu, H. H. Zeng and S. P. Yan, *J. Inorg. Biochem*.,2011, **105**, 894.
13 (a)P. Scott and S. E. Howson, *Dalton Trans.*, 2011, 40, 10268; (b) J. Crassous, *Chem. Commun.*, 2012, **48**, 9684.
14 (a) A. Malviya, H. S. Jena, A. K. Mondal and S. Konar, *Eur. J. Inorg. Chem.*, 2015, 2901; (b) B. Wang, Z. Zang, H. Wang, W. Dou, X. Tang, W. Liu, Y. Shao, J. Ma, Y. Li and Z. Zhou, *Angew Chem. Int. Ed.* 2013, **52**, 3756; (c) A. K. Mondal, H. S. Jena, A. Malviya and S. Konar, *Inorg. Chem*., 2016, **55**, 5237.
15 (a) C. Zimm, A. Jastrab, A. Sternberg, V. Pecharsky, K. A. Gschneidner Jr., M. Osborne and I. Anderson, *Adv. Cryog. Eng.*, 1998, **43**, 1759; (b) V. Pecharsky and K. A. Gschneidner Jr., *J. Magn. Magn. Mater.*, 1999, **200**, 44.
16 A. Adhikary, H. S. Jena, S.Konar, Dalton Trans., 2015, **44**, 15531.
17 *SAINT, SAX Area-Detector Integration Program*, v6.22, Bruker AXS Inc., Madison, WI, 1997-2001.
18 G. M. Sheldrick, SADABS, *Program for Absorption Correction of Area Detector Frames*, Bruker AXS Inc., Madison, WI, 2008.
19 (a) G. M. Sheldrick, *SHELXL-2014*, *Program for Crystal Structure Renement*, University of Göttingen, Göttingen, Germany,2014.http://shelx.uni-ac.gwdg.de/SHELX/index.php. (b) L. J. Farrugia, J. Appl. Cryst. 2012,**45**, 849. (c)O. V. Dolomanov, L. J. Bourhis, R. J. Gildea, J. A. K. Howard, H. Puschmann, 2009,*J. Appl Cryst*. **42**, 229.
20 A. L. Spek, *Acta Cryst*.2015, **C71**, 9.
21 A. L. Spek, *Acta Cryst*. 2009, **D65**, 148.
22 W. Liu and H. H. Thorp, *Inorg. Chem*.,1993, **32**, 4102.
23 U. Golla and S. S. Bhimathati, *Scientific World Journal***,**2014, 215084.
24 U. Golla, G. Bandi and R. S. Tomar, *Chem. Res. Toxicol.*, 2015, **28**, 1246.
25 I. M. Ghobrial, T. E. Witzig and A. A. Adjei, *CA: a cancer journal for clinicians*,2005, **55**, 178.
26 P. R. Walker, S. Pandey and M. Sikorska, *Cell death and differentiation*,1995, **2**, 97.
27 (*a*) F. Cui, S. Li, C. Jia, J. S. Mathieson, L. Cronin, X.-J. Yang and B. Wu, *Inorg. Chem*.,2012, **51**, 179; (*b*) J. L. Sessler, P. A. Gale and W.-S. Cho, *Anion Receptor Chemistry; Royal Society of Chemistry*: Cambridge, U.K., 2006; (*c*) E. A. Katayev, Y. A. Ustynyuk and J. L. Sessler, *Coord. Chem. Rev*.,2006, **250**, 3004; (*d*) S. O. Kang, R. A. Begum and K. B.-James, *Angew. Chem., Int. Ed*.,2006, **45**, 7882; (*e*) C. Caltagirone and P. A. Gale, *Chem. Soc. Rev*.,2009, **38**, 520; (*f*) P. A. Gale, S. E. García-Garrido andJ. Garric,*Chem. Soc. Rev*.,2008, **37**, 151; (*g*) K. M. Mullen and P. D. Beer, *Chem. Soc. Rev.*,2009, **38**, 1701; (*h*) J. W. Steed, *Chem. Soc. Rev*.,2009, **38**, 506; (*i*) V. Amendola and L. Fabbrizzi, *Chem. Commun.*,2009, 513; *(j*) L. P. Harding, J. C. Jeffery, T. Riis-Johannessen, C. R. Rice and Z. Zeng, *Dalton Trans*.,2004, 2396.
28 A. Mori, T. Suzuki, Y. Nakatani, Y. Sunatsuki, M. Kojima and K. Nakajima, *Dalton Trans.* 2015, **44**, 15757.
29 (*a*) N. Mondal, D. K. Dey, S. Mitra and K. M. A. Malik, *Polyhedron,*2000, **19**, 2707; (*b*) N. Heinrich, W. Koch, G. Frenking and H. Schwarz, *J. Am. Chem. Soc*.,1986, **108**, 593; (*c*)A. J. Deeming, P. J. Manning, I. P. Rothwell, M. B. Hursthouse and N. P. C. Walker, *J. Chem. Soc., Dalton Trans*.,1984, 2039.
30 (*a*) M. H. Zeng, Y. L. Zhou, M. C. Wu, H. L. Sun and M. Du, *Inorg. Chem*.,2010, **49**, 6436; (*b*) J. S. Miller and M. Drillon, *Magnetism: Molecule to Materials V*; Wiley-VCH: Weinheim, Germany, 2005, 347; (*c*) R. X. Yao, Y. L. Qin, F. Ji, Y. F. Zhao and X. M. Zhang, *Dalton Trans*.,2013,**42**, 6611.
31 R. -X. Yao, Y. -L. Qin, F. Ji, Y. -F. Zhao and X. -M. Zhang, *Dalton Trans*.,2013, **42**, 6611.
32 X.-J. Song, Md. Muddassir, Y. Chen, H.-S. Wang, Y. Song and X. Z. You, *Dalton Trans*.,2013, **42**, 1116.
33 Y. -Z. Zheng, W. Xue, M.- L. Tong, X. -M. Chen; F. Grandjeanand G. J. Long, *Inorg. Chem*.,2008, **47**, 4077.
34 (*a*) S. Y. Lin, G. F. Xu, L. Zhao, Y. N. Guo, Y. Guo and J. Tang, *Dalton Trans*.,2011, **40**, 8213; (*b*) J. Bartolomé, G. Filoti, V. Kuncser, G. Schinteie, V. Mereacre, C. E. Anson, A. K. Powell, D. Prodius and C. Turta, *Phys. Rev. B: Condens. Matter*,2009, **80**, 014430.
35 (*a*) J. W. Sharples, Y. Z. Zheng, F. Tuna, E. J. L. McInnes and D. Collison, *Chem. Commun*.,2011, **47**, 7650; (*b*) R. Shaw, R. H. Laye, L. F. Jones, D. M. Low, C. T. Eeckelaers, Q. Wei, C. J. Milios, S. Teat, M. Helliwell, J. Raftery, M. Evangelisti, M. Affronte, D. Collison, E. K. Brechin and E. J. L. McInnes, *Inorg. Chem*.,2007, **46**, 4968; (*c*) M. Evangelisti, A. Candini, A. Ghirri, M. Affronte, E. K. Brechin and E. J. L. McInnes, *Appl. Phys. Lett*.,2005, **87**, 072504; (*d*) Z. G. Wang, J. Lu, C. Y. Gao, C. Wang, J. L. Tian, W. Gu, X. Liu and S. P. Yan, *Inorg. Chem. Commun.*,2013, **27**, 127; (*e*) N. Ishikawa, M. Sugita, T. Ishikawa, S. Y. Koshihara and Y. J. Kaizu, *J. Phys. Chem. B***,**2004, **108**, 11265; *(f*) G. Aromi and E. K. Brechin, *Struct. Bonding*, 2006, **122**, 1; (*g*) M. Evangelisti and E. K. Brechin, *Dalton Trans*.,2010, **39**, 4672; (*h*) G. Karotsis, M. Evangelisti, S. J. Dalgarno and E. K. Brechin, *Angew. Chem., Int. Ed.*,2009, **48**, 9928; (*i*) Y. Z. Zheng, M. Evangelisti and R. E. P. Winpenny, *Chem. Sci*.,2011, **2**, 99.
36 (*a*) Z. Chen, B. Zhao, P. Cheng, X. Q. Zhao, W. Shi and Y. Song, *Inorg. Chem*.,2009, **48**, 3493; (*b*) J. X. Xu, Y. Ma, D. Z. Liao, G. F. Xu, J. Tang, C. Wang, N. Zhou, S. P. Yan, P. Cheng and L. C. Li, *Inorg. Chem*.,2009, **48**, 8890; (*c*) Y. N. Guo, X. H. Chen, S. Xue and J. Tang, *Inorg. Chem*.,2011, **50**, 9705; (*d*) Y. Z. Zheng, Y. Lan, C. E. Anson and A. K. Powell, *Inorg. Chem.,*2008, **47**, 10813; (*e*) A. K. Mondal, S. Goswami and S. Konar, *Dalton Trans*.,2015, **44**, 5086; (*f*) L. Zou, L. Zhao, P. Chen, Y. N. Guo, Y. Guo, Y. H. Lib and J. Tang, *Dalton Trans.,*2010, **41**, 2966.
37 (*a*) L. G. Westin, M. Kritikos and A. Caneschi, *Chem. Commun.*,2003, 1012; (*b*) P. H. Lin, T. J. Burchell, L. Ungur, L. F. Chibotaru, W. Wernsdorfer and M. Murugesu, *Angew. Chem., Int. Ed.*,2009, **48**, 9489; (*c*) J. Tang, I. Hewitt, N. T. Madhu, G. Chastanet, W. Wernsdorfer, C. E. Anson, C. Benelli, R. Sessoli and A. K. Powell, *Angew. Chem., Int. Ed.,*2006, **45**, 1729; (*d*) S. K. Langley, B. Moubaraki, C. M. Forsyth, I. A. Gass and K. S. Murray, *Dalton Trans*.,2010, **39**, 1705; (*e*) I. J. Hewitt, Y. H. Lan, C. E. Anson, J. Luzon, R. Sessoli and A. K. Powell, *Chem. Commun.***,**2009, 6765; (*f*) P. H. Lin, T. J. Burchell, R. Clerac and M. Murugesu, *Angew. Chem., Int. Ed.***,**2008, **47**, 8848; (*g*) M. T. Gamer, Y. Lan, P. W. Roesky, A. K. Powell and R. Clerac, *Inorg. Chem*.,2008, **47**, 6581; (*h*) J. Tang, I. Hewitt, N. T. Madhu, G. Chastanet, W. Wernsdorfer, C. E. Anson, C. Benelli, R. Sessoli and A. K. Powell, *Angew. Chem., Int. Ed*.,2006, **45**, 1729; (*i*) G. F. Xu, Q. L. Wang, P. Gamez, Y. Ma, R. Clerac, J. Tang, S. P. Yan, P. Cheng and D. Z. Liao, *Chem. Commun*.,2010, **46**, 1506; (*j*) Y. Wang, X. L. Li, T. W. Wang, Y. Song and X. Z. You, *Inorg. Chem*.,2010, **49**, 969; (*k*) B. Hussain, D. Savard, T. J. Burchell, W. Wernsdorfer and M. Murugesu, *Chem. Commun.***,**2009, 1100.
38 K. S. Cole and R. H. Cole, *J. Chem. Phys*.,1941, **9**, 341.
39 (*a*) Q.L. Zhang, J.G. Liu, H. Chao, G. Q. Xue and L.N. Ji,*J. Inorg. Biochem.*, 2001,**83,** 49; (*b*) A. Oleksi, A.G. Blanco, R. Boer, J. Usón, J. Aymamí, A. Rodger, M. J. Hannon and M. Coll,*Angew. Chem. Int. Ed.*, 2006,**45**, 1227.

View Article Online
DOI: 10.1039/C6DT01496H

40 (*a*) J. K. Barton, A. T. Danishefsky and J. M. Goldberg, *J. Am. Chem. Soc.*, 1984, **106**, 2172; (*b*) S. A. Tysoe, R. J. Morgan, A. D. Baker and T. C. Strekas, *J. Phys. Chem.*, 1993, **97**, 1707.
41 Q. Li, P. Yang, H. Wang and M. Guo, *J. Inorg. Biochem.*, 1996, **64**, 181.
42 (a) J. K. Barton, A. T. Danishefsky and J. M. Goldberg, *J. Am. Chem. Soc.*, 1984, **106**, 2172; (b) C. S. Chow and J. K. Barton, *Methods Enzymol.*, 1992, **212**, 219.
43 R. S. Kumar, S. Arunachalam, V. S. Periasamy, C. P. Preethy, A. Riyasdeen and M. A. Akbarsha, *Polyhedron*, 2008, **27**, 1111.
44 B. H. Geierstanger, M. Mrksich, P. B. Dervan and D. E. Wemmer, *Science*,1994, **266**, 646.
45 J. L. G.-Gimenez, G. Alzuet, M. G.-Alvarez, A. Castineiras, M. L.-Gonzalez and J. Borras, *Inorg. Chem*.,2007,**46**, 7178.
46 L. Tjioe, T. Joshi, J. Brugger, B. Graham and L. Spiccia, *Inorg. chem.*,2011, **50**, 621.
47 S. Imbeaud, E. Graudens, V. Boulanger, X. Barlet, P. Zaborski, E. Eveno, O. Mueller, A. Schroeder and C. Auffray, *Nucl. Acids Res.*, 2005, **33**,e56.
48 M. J. Li, T. Y. Lan, X. H. Cao, H. H. Yang, Y. Shi, C. Yi and G. N. Chen, *Dalton Trans*.,2014, **43**, 2789.
49 M. Kajstura, H. D. Halicka, J. Pryjma and Z. Darzynkiewicz, *Cytometry Part A***,**2007, **71**, 125.
50 T. Zhang, X. Chen, L. Qu, J. Wu, R. Cui and Y. Zhao, *Bioorganic & medicinal chemistry***,**2004, **12**, 6097.
51 I. Vermes, C. Haanen, H. S.-Nakken and C. Reutelingsperger, *Journal of immunological methods*,1995,**184**, 39.
52 Z. Darzynkiewicz, S. Bruno, G. D. Bino, W. Gorczyca, M. A. Hotz, P. Lassota and F. Traganos, *Cytometry,*1992, **13**, 795.
53 (*a*) H. D. Halicka, E. Bedner and Z. Darzynkiewicz,*Experimental cell research***,**2000, **260**, 248; (*b*) P. R. Walker, L. Kokileva, J. LeBlanc and M. Sikorska, *Bio Techniques*,1993, **15**, 1032.

View Article Online
DOI: 10.1039/C6DT01496H

Journal Name

ARTICLE

Table of Content

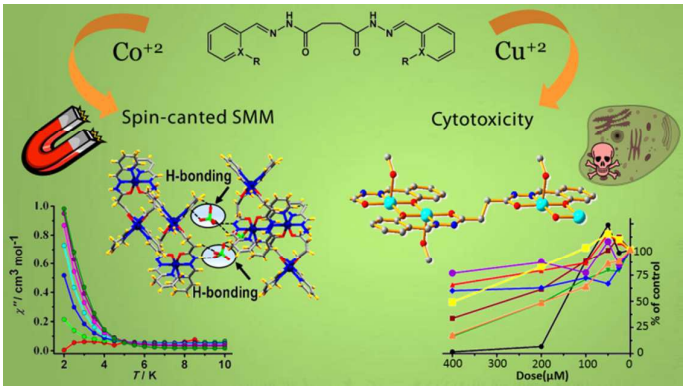

Three double stranded helicates[$Cu^{II}_2(H_2L^1)(HL^1)$] $(ClO_4)_3 \cdot H_2O$ (**1**), [$Co^{II}_2(H_2L^1)_2$]$(ClO_4)_4$ (**3**), [$Co^{II}_2(H_2L^2)_2$] $\cdot 2\ H_2O$ (**4**) and one linear chain compound [$Cu^{II}_2(H_2L^2)(CH_3OH)_2$] $(ClO_4)_2 \cdot 2\ CH_3OH$ (**2**) have been synthesized following similar synthetic strategy with a mere change in the coordination of the ligands. Magnetic study of compound **3** reveals spin-canting and long range magnetic ordering at low temperature regime induced by hydrogen bonding interaction. Ac magnetic susceptibility data also shows slow relaxation of magnetization. The compound **3** is one of the rare examples which shows both spin canting and slow relaxation of magnetization induced by H-bonding. DNA nicking studies showed that all the compounds **1**-**4** significantly cleave the pUC19 plasmid DNA. Nuclease activity of the compounds was also boosted in presence of H_2O_2. Cu-based compounds **1** and **2** exhibited significant cytotoxicity on mammalian cancer cell lines.